Atomic-Scale Dynamics of Surface-Catalyzed Hydrogenation/ Dehydrogenation: NH on Pt(111)

Zhu Liang,[†] Hyun Jin Yang,[‡] Junepyo Oh,[‡] Jaehoon Jung,[‡,§] Yousoo Kim,*,[‡] and Michael Trenary*,[†]

[†]Department of Chemistry, University of Illinois at Chicago, 845 West Taylor Street, Chicago, Illinois 60607, United States, [‡]Surface and Interface Science Laboratory, RIKEN, 2-1 Hirosawa, Wako-shi, Saitama 351-0198, Japan, and [§]Department of Chemistry, University of Ulsan, 93 Daehak-ro, Nam-gu, Ulsan 680-749, Republic of Korea

ABSTRACT Low-temperature scanning tunneling microscopy (LT-STM) was used to move hydrogen atoms and dissociate NH molecules on a Pt(111) surface covered with an ordered array of nitrogen atoms in a (2 × 2) structure. The N-covered Pt(111) surface was prepared by ammonia oxydehydrogenation, which was achieved by annealing an ammonia—oxygen overlayer to 400 K. Exposing the N-covered surface to $H_2(g)$ forms H atoms and NH molecules. The NH molecules occupy face-centered cubic hollow sites, while the H atoms occupy atop sites. The STM tip was used to dissociate NH and to induce hopping of H atoms. Action spectra consisting of the reaction yield *versus* applied bias voltage were recorded for both processes, which revealed that they are vibrationally mediated. The threshold voltages for NH dissociation and H hopping were found to be 430 and 272 meV, corresponding to the excitation energy of the N—H stretching and the Pt—H stretching modes, respectively. Substituting H with D results in an isotopic shift of −110 and −84 meV for the threshold voltages for ND dissociation and D hopping, respectively. This further supports the conclusion that these processes are vibrationally mediated.
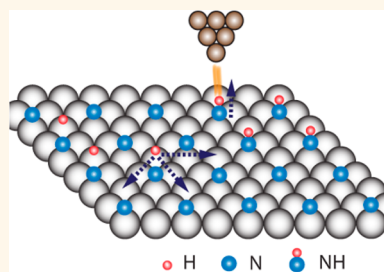
KEYWORDS: Pt(111) · NH dissociation · H hopping · low-temperature scanning tunneling microscopy · action spectroscopy

The interaction of hydrogen with metal surfaces has been studied for decades and is still of great interest for its role in hydrogenation reactions, hydrogen storage, and fuel cells. Hydrogen atoms on metal surfaces are difficult to detect by many surface science techniques because hydrogen is such a poor electron scatterer. Since the first scanning tunneling microscope (STM) was developed by Binnig and Rohrer in the early 1980s,[1,2] it has been a powerful tool for understanding the structure and properties of materials at the atomic scale. The "invisible" hydrogen atom can be imaged by STM on various metal surfaces. Tatarkhanov *et al.* reported that H appears as a depression on Ru(0001) and forms different ordered structures as a function of coverage.[3] Similar observations were found by Mitsui and co-workers in their study of hydrogen adsorbed on Pd(111).[4] In general, the reduced thermal broadening at cryogenic temperatures provides sufficient resolution for vibrational spectroscopy of single molecules or even of single H atoms. The method known as STM inelastic electron

tunneling spectroscopy (STM-IETS) is based on the idea that tunneling electrons from the STM tip can excite a specific vibrational mode of an adsorbate and can be observed as peaks in d^2I/dV^2 spectra at energies corresponding to the vibrational modes. Lauhon and Ho used STM-IETS to characterize the vibrational modes of hydrogen on Cu(001), where they detected H—Cu and D—Cu stretch (vertical) modes but not the hindered translations (parallel) in IETS spectra.[5] Fernández-Torres and co-workers measured H—Pd vibrations of hydrogen on Pd(111) and observed both vertical and parallel modes.[6] A drawback of STM-IETS is that the selection rules are unclear due to the complex relationship between inelastic and elastic contributions to the total tunneling current.[7−9] In addition to measuring the vibrational modes, motion of H on metal surfaces can be induced by thermal and tip-electron activation. In both cases, time-lapse STM images were used to investigate the diffusion rate of hydrogen atoms on surfaces. Thermally activated diffusion of H(D) on Cu(001)[5] was investigated at temperatures

between 9 and 80 K. Tunneling activated diffusion of H on Pd(111)[6] and H(D) on Cu(111)[10] was studied at 5 K. Tip-induced motion is expected because excitation of the vibrational modes by tunneling electrons can induce motion of the atom or molecule by dissipating the energy to another mode corresponding to the reaction coordinate. As the tip can be precisely positioned over a specific atom or molecule on the surface, manipulating individual atoms or molecules is readily achieved *via* STM. There are many examples of tip-induced lateral (atom/molecule diffusion across the surface) and vertical transitions (where an atom/molecule is picked up by the tip).[11] In addition to time-lapse STM images, another method to investigate tunneling electron-induced motion is known as "action spectroscopy", which was introduced by Sainoo *et al.* in studying the configuration change of *cis*-2-butene on Pd(110).[12] The instrumentation, theoretical aspects, and experimental demonstrations of STM-AS have been reviewed recently.[13] Briefly, measurement of the induced motion *versus* applied bias voltage generates the "action spectrum (AS)", which reveals threshold voltages due to excitation of the vibrational modes responsible for inducing a given motion. The theoretical model developed by Ueba and co-workers provides a basis for extracting parameters from fits to the measured action spectra.[9,14−16] With STM-AS, vibrational modes can be detected that may not be observable with IETS.[7,8] Also, it provides information on the mechanism of the motion. In the present study, we characterized the atomic structure of H and NH on a N-covered Pt surface. In addition, we investigated hydrogen atom hopping and NH dissociation (NH → N + H) using STM-AS.

RESULTS AND DISCUSSION

Atomic Hydrogen on p(2 × 2)-N/Pt(111). Hydrogen atoms on an otherwise clean surface usually appear as depressions and occupy face-centered cubic (fcc) hollow sites as revealed by STM.[3,5,6] Other impurities, such as oxygen and carbon atoms, also appear as depressions.[17] Thus, at very low coverages, it is difficult to distinguish H atoms from impurities in a topographic image. In contrast, we found that hydrogen atoms appear as protrusions on a N-covered Pt(111) surface, making them readily observable even at very low coverages. Figure 1a shows the honeycomb structure of the p(2 × 2)-N phase on Pt(111), which was discussed in detail earlier.[18] In this structure, Pt atoms that are not adjacent to N atoms are visible in the STM images and form a (2 × 2)-Pt lattice and are referred to as Pt-visible, whereas Pt atoms that are bonded to N atoms are referred to as Pt-invisible because they are not resolved. Such a (2 × 2)-Pt lattice serves as a well-ordered template for H adsorption. After exposing the N-covered surface to H₂(g) at 50 K, H atoms are seen as protrusions (Figure 1b,c) and are separated by two Pt

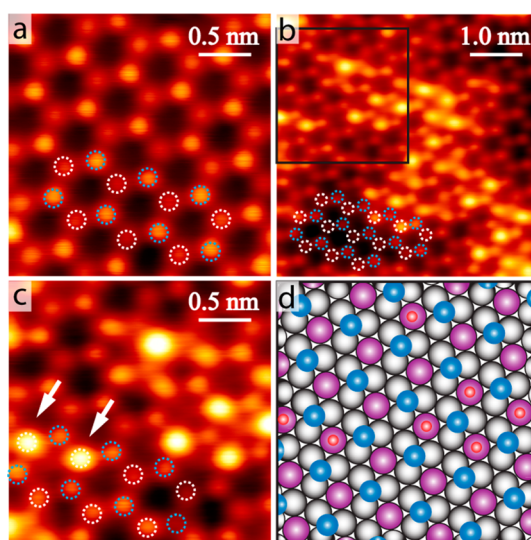**Figure 1.** (a) Honeycomb structure of p(2 × 2)-N (2.5 nm × 2.5 nm, V_s = 5 mV, I_t = 1 nA). (b) Hydrogen atoms adsorbed on p(2 × 2)-N (5 nm × 5 nm, V_s = 5 mV, I_t = 1 nA). (c) Zoomed-in image of the black square in (b) (2.5 nm × 2.5 nm, V_s = 5 mV, I_t = 1 nA). White arrows indicate H atoms. (a−c) Blue and white circles indicate N and Pt atoms, respectively. (d) Model showing H atoms adsorbed on p(2 × 2)-N corresponding to (c). Gray, Pt-invisible; purple, Pt-visible; blue, N atom; red, H atom.

lattice constants from each other. White circles superimposed on the images in Figure 1a−c indicate the Pt where the H atoms can adsorb. The presence of N shifts the most stable binding site for H from a hollow to an atop site. It is similar to when H adsorbs on p(2 × 2)-O on Pt(111), where density functional theory (DFT) calculations have shown that the atop sites are favored.[19,20] Figure 1d shows the model corresponding to Figure 1c, where Pt-visible is colored purple and Pt-invisible gray. The H and N atoms are shown as red and blue, respectively. The separation of H atoms by the honeycomb structure minimizes the interaction among neighbors and limits the formation of H dimers or larger clusters as observed on Cu(111).[10] The p(2 × 2)-N/Pt(111) surface thus serves as an ideal system for manipulating individual H atoms.

NH on p(2 × 2)-N/Pt(111). Annealing the surface with adsorbed hydrogen to 300 K leads to the formation of NH, which is characterized by a triangular shape, as indicated by the blue arrow in Figure 2e,f. Occasionally, with an unstable tip, the triangular shape of the NH molecules is lost (see Figure 5a), whereas residual NH₃ molecules appear with a three-lobed structure. With a normal stable tip, NH₃ molecules appear as round and bright protrusions. Images showing these effects are presented in the Supporting Information. Regardless of the tip state, ammonia molecules always occupy atop sites. Protrusions due to hydrogen atoms are also observed (white arrows in Figure 2e,f). Note that a small amount of NH and H can also be found on the surface after the oxydehydrogenation of ammonia
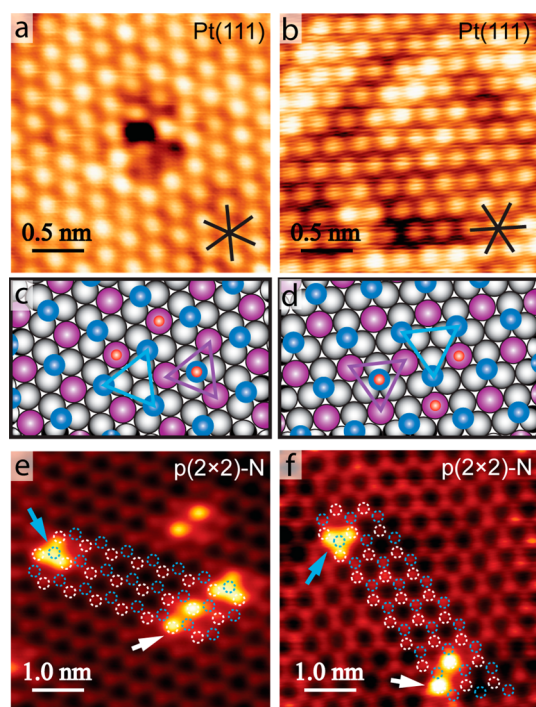
Figure 2. (a,b) STM images of clean Pt(111) surfaces of two different azimuthal orientations [(a) 2.5 nm × 2.5 nm, V_s = 2 mV, I_t = 6 nA; (b) 2.5 nm × 2.5 nm, V_s = 2 mV, I_t = 6 nA]. (c,d) Model of p(2 × 2)-N/Pt(111) corresponding to the orientations in (a) and (b). Gray, Pt-invisible; purple, Pt-visible in honeycomb; blue, N atom; red, H atom. Blue and purple triangles indicate the half unit cell of N(2 × 2) and Pt(2 × 2), respectively. (e,f) STM image of NH and H on p(2 × 2)-N/Pt(111). Blue and white arrows indicate an NH molecule and a H atom, respectively. A honeycomb lattice is superimposed on the p(2 × 2)-N structure, with blue and white circles indicating N and Pt atoms, respectively [(e) 5 nm × 5 nm, V_s = 100 mV, I_t = 0.5 nA; (f) 5 nm × 5 nm, V_s = 50 mV, I_t = 1 nA].

when ammonia is present in slight excess. Nevertheless, the appearance of NH and H is not affected by how they are formed. To demonstrate the reproducibility, as well as to clarify the appearance of triangular NH molecules, two sets of images are presented in Figure 2. The left and right panels correspond to the results obtained on two different crystals with different azimuthal orientations with respect to the piezo scanner. Other than that, the images are identical. The triangular-shaped NH molecules occupy fcc hollow sites, as do the N atoms. Figure 2a,b shows atomically resolved images of clean Pt(111), which help to assign the lattice orientation. Figure 2c,d shows models of the p(2 × 2)-N structure drawn according to the orientation of each single crystal, which facilitates the interpretation of the adsorption sites in the other images. The half unit cells of the (2 × 2)-N (blue) and (2 × 2)-Pt (purple) structures are shown, which are the up- and down-pointing triangles centered at a hollow site (blue triangle) or a nitrogen atom (purple triangle), respectively. Such up- and down-pointing triangles reflect the azimuthal orientations of the crystal. The triangular shape of the molecule can be understood as the perturbation of the

electronic properties of the nearest Pt atoms by the NH. As illustrated in Figure 2e,f, the triangle is centered at the NH molecule and spreads to the three nearest "visible" Pt atoms. Hydrogen atoms, although present in pairs in the two images shown in Figure 2, are not necessarily always present in pairs, and single H atoms and groups of more than two are also observed (see Figure 1b).

In Figure 3, we show simulated STM images for p(2 × 2)-N/Pt(111) obtained from DFT calculations using the Vienna *ab initio* simulation package (VASP),[21,22] in which ion−electron interactions are described by projector-augmented wave (PAW) pseudopotentials[23,24] and the exchange-correlation is described by the Perdew−Burke−Ernzerhof (PBE) approximation.[25] The Pt(111) surface was modeled with a (6 × 6) supercell of six layers with the bottom two layers fixed and the other four layers relaxed. Only the fcc hollow site was considered for nitrogen adsorption. The surface irreducible Brillouin zone was sampled with 4 × 4 × 1 Γ-centered grids. The cutoff energy of the plane wave expansion was 400 eV. The Tersoff−Hamann scheme[26,27] was used to simulate the STM images from DFT calculations. As shown in the top panel of Figure 3, no specific bias dependence was observed for p(2 × 2)-N/Pt(111) from 0.05 to 0.20 eV. The honeycomb structure in the simulated STM images agrees well with the experimental results (Figure 1a). The simulated appearance of isolated NH molecules for an assumed p(6 × 6)-NH layer are shown in Figure 3e−h. The triangular shape of an NH molecule agrees well with the experimental results.

After exposing the nitrogen-covered surface to $H_2(g)$ at 300 K, we observed an increase in the number of NH molecules, as shown in Figure 4. Before exposure to $H_2(g)$, there are several residual NH molecules on the surface, as indicated by blue arrows in Figure 4a. Hydrogen atoms are also present on the surface, one of which is indicated by the white arrow, which is consistent with other STM images. Note that the brightest protrusions are residual ammonia molecules as discussed earlier.[18] The images in Figure 4b−d show the topography of the surface after exposure to $H_2(g)$. Two types of NH molecules are clearly distinguished by their appearances: isolated molecules and molecules that are part of an island. Isolated NH molecules are easily identified by their characteristic triangular shape. Islands of NH molecules, however, have the same general appearance as p(2 × 2)-N. The atomically resolved image inside the island shows a well-ordered (2 × 2) structure (Figure 4c,d). The bright dots inside the island correspond to the Pt(2 × 2) lattice, which can be identified by expanding the Pt lattice from the p(2 × 2)-N areas (where the Pt and N atoms can be distinguished and labeled accordingly) to the (2 × 2)-NH island. As shown in Figure 4d, the black grid indicates the Pt(2 × 2) lattice and matches the positions
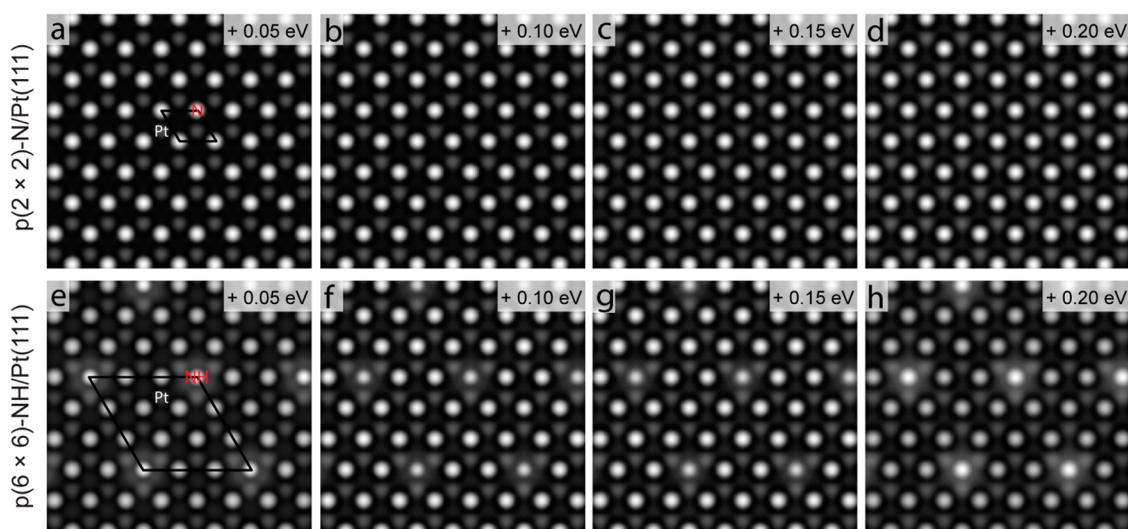
Figure 3. (a–d) Simulated STM images with an iso-surface level of 0.05 e/bohr^3 of p(2 × 2)-N/Pt(111) for the indicated bias voltages. (e–h) Simulated STM images of p(6 × 6)-NH/Pt(111). Unit cells and the positions of Pt, N, and NH are indicated in (a) and (e).

of the bright dots. NH vacancies inside the island appear as holes and are located at the hollow sites of the (2 × 2) lattice grid. The Pt atoms are labeled as white circles, and the NH molecules as blue circles in Figure 4d. The detailed structure within the NH island is thus resolved. There are very few NH islands present on the surface, and they are found to grow to large sizes, up to 40 nm × 40 nm.

The formation of NH islands and isolated NH molecules indicate an inhomogeneous hydrogenation process. One previous RAIRS study found that at the saturation coverage of NH, only about 60–68% of the surface N atoms were converted to NH,[28] whereas another RAIRS study revealed that the formation of NH follows first-order kinetics at 200 K,[29] implying that the effective rate of NH formation is independent of the hydrogen coverage and depends solely on the nitrogen coverage. This is consistent with the high mobility of hydrogen on the surface.[29] In other words, the reaction of $N_{ad} + H_{ad} \rightarrow NH_{ad}$ proceeds as long as there is some hydrogen present on the surface. If the hydrogen coverage does not affect the rate of NH formation and the N atoms are homogeneous across the surface in the p(2 × 2) phase, the origin of the inhomogeneous NH distribution presumably lies in the H_2 dissociative adsorption dynamics. Molecular hydrogen adsorbs on the Pt(111) surface with a low initial dissociative sticking probability of 0.1 at 150 K,[30] and the presence of atomic nitrogen[31] presumably further suppresses it, as has been found on Ru(0001),[32] Ni(100),[33] and Pt(110).[34] Similar suppression of hydrogen uptake has been observed on oxygen-covered Pt(111).[35] A molecular dynamics study of the hydrogen dissociation on p(2 × 2)-O/Pt(111) indicates that dissociation preferentially occurs on top of the Pt atoms that are not bonded to adsorbed oxygen atoms.

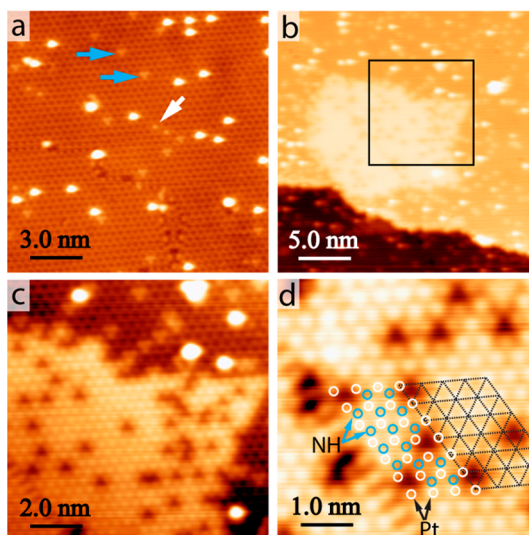**Figure 4.** (a) STM image of p(2 × 2)-N before exposure to H_2(g) (15 nm × 15 nm, V_s = 100 mV, I_t = 1 nA). (b–d) STM images of an NH island after exposure to H_2(g) [(b) 50 nm × 50 nm, V_s = 50 mV, I_t = 1 nA; (c) 10 nm × 10 nm, V_s = 50 mV, I_t = 1 nA; (d) 5 nm × 5 nm, V_s = 50 mV, I_t = 1 nA].

In addition, the most stable binding site for a H atom shifts from the hollow site (on the clean surface) to the atop site in the presence of a p(2 × 2)-O layer.[19] Extrapolating these results to the p(2 × 2)-N-covered surface, we assume that the atop sites of the visible Pt atoms are where H_2 dissociation and H adsorption occur. The situation is different at the steps, where higher reactivity is generally observed because of a stronger adsorbate–substrate interaction at low-coordination sites. Studies of hydrogen dissociation on stepped Pt surfaces indicate that, in addition to direct dissociation on the terraces, an indirect channel appears at low kinetic energy.[36] The influence of "indirect" and
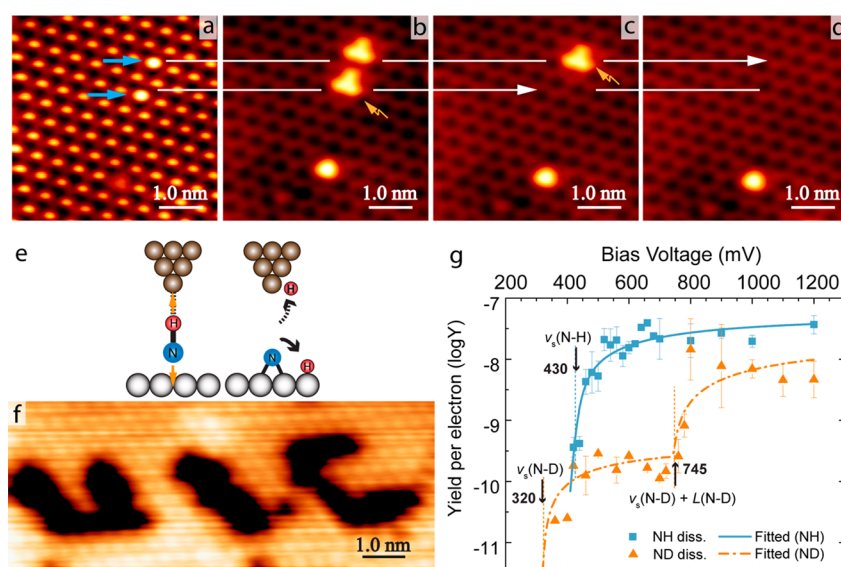
Figure 5. (a,b) STM images of NH molecules on p(2 × 2)-N under different tip states (5 nm × 5 nm, V_s = 80 mV, I_t = 0.6 nA). (c,d) STM images of the dissociation of isolated NH molecules (5 nm × 5 nm, V_s = 80 mV, I_t = 0.6 nA). (e) Models showing NH dissociation induced by tunneling electrons. (f) "UIC" formed by selective dissociation of NH molecules (20 nm × 10 nm, V_s = 50 mV, I_t = 1 nA). (g) Action spectra of NH (blue)/ND (orange) dissociation.

"direct" dissociative sticking probabilities (S_{indir} and S_{dir}) in the development of surface structures has been discussed by Salanov and co-authors.[37,38] In their Monte Carlo simulations, at $S_{indir}/S_{dir} \geq$ 1.0, island-forming adsorption dominates. The concentration of the islands is low, but their size is large. In our case, if the indirect channel predominates at the steps, then NH islands would form there, whereas the direct channel is more important on the terraces leading to isolated NH molecules. This is consistent with our observation of a low density of large NH islands, which seem to be preferentially located near the Pt steps.

The dynamics of H_2 dissociation on p(2 × 2)-N on Pt(111) also explains why only about 60% of the surface N can be converted to NH. Because the adsorbed nitrogen atoms reduce the activity of the nearest neighbor "invisible" Pt atoms, it is reasonable to assume that most of the dissociative adsorption on the terraces occurs at the "visible" Pt atom on the p(2 × 2)-N surface. Forming an NH molecule alters the electronic properties of those "visible" Pt atoms, as can be seen by the triangular shape in the STM images. The active Pt atoms are thus deactivated by forming an NH molecule, similar to a site-blocking effect. Due to the small size of NH compared to that of the Pt atom, it is not a spatial blocking but more of an electronic effect and possibly may increase the barrier to H_2 dissociation. Once the active Pt atoms are deactivated, the direct channel of H_2 adsorption is locally blocked around an NH molecule. As a result, a H_2 molecule has to find an active Pt atom somewhere else to dissociate, and then a H atom can diffuse across the surface until reacting with a N atom. Moreover, hydrogenation of atomic

N does not proceed beyond NH on Pt(111). DFT calculations found that the reaction barrier for N + H → NH on Pt(111) is less than 1.0 eV (0.66 eV reported by Mudiyanselage et al.[29] and 0.94 eV reported by Michaelides and Hu[39]), while a 1.31 eV reaction barrier was reported for NH + H → NH_2 on Pt(111).[39] Thus, adding a second H atom to form NH_2 is not achievable, and the absence of NH_2 precludes NH_3 formation. Consequently, there is no outlet channel for a product like NH_3 to desorb from the surface, which means the active site for H_2 dissociation cannot be recovered. As the hydrogenation proceeds and the coverage of NH increases, fewer and fewer sites are available for H_2 to dissociate via the direct channel. Because one NH molecule blocks three Pt atop sites, an ideal surface (no defects or steps) is completely blocked for H_2 dissociation when 1/3 of the N is converted to NH. Thus, the ~60% conversion from N to NH observed in RAIRS and XPS[28] is a combination of 33% conversion on terraces (N converts to scattered NH) and 100% conversion near step edges (N converts to NH islands). The actual percent conversion between 33 and 100% will then depend on the step density.

NH Dissociation Induced by Tunneling Electron. An NH molecule can be imaged differently under different tip states. It appears as a bright protrusion under a modified tip and changes to a triangular shape with a clean tip, as shown in Figures 5a (modified tip) and 5b (clean tip). Although a modified tip generally provides better image resolution, a clean tip is used for measuring action spectra because it is more stable for spectroscopy measurements. Figure 5b−d shows a series of images taken in the process of dissociating individual NH molecules. Two NH molecules are indicated by blue

arrows in Figure 5a and are imaged with a modified tip. Scanning the same area with a clean tip generated the image in Figure 5b, which shows triangle-shaped NH molecules. When the tip was placed above the NH molecule indicated by the yellow arrow in Figure 5b and a pulse of 0.7 V and 1 nA for 4 s was applied, the H atom was removed from the NH, as shown in Figure 5c. Applying the same pulse to the NH molecule on the right in Figure 5c removed that H atom, as well. An unperturbed p(2 × 2)-N structure is observed after dissociating both NH molecules, as shown in Figure 5d.

Figure 5e illustrates the tip-induced dissociation of NH. Measured action spectra are shown in Figure 5g, where both the experimental data (blue squares) and the fitted spectrum (blue curve) are shown. A threshold energy of 430 meV for NH dissociation is observed, which is comparable to the values of v_s(N−H) obtained from a theoretical calculation (427 meV)[40] and an experimental measurement (411 meV).[28] The action spectrum for ND dissociation shows two thresholds, at 320 and 745 meV. The vibrational mode associated with 320 meV is the ND internal stretch (v_s(N−D)), with an isotopic shift of −110 meV compared to v_s(N−H). The value of 745 meV corresponds to a combination of the internal stretch and frustrated rotation ($2v_s$(N−D) + L(N−D)). As suggested by Figure 5e, the H atom produced upon NH dissociation can either adsorb on the surface outside of the imaging area or transfer to the tip. It is unlikely that the H atom would desorb from the surface for the bias voltages used because the binding energy of H on Pt(111) is calculated to be 2.7 eV.[40]

Hydrogen Hopping Induced by Tunneling Electrons. It is relatively easy to observe tip-induced hopping of H atoms in this system because H sits on top of a Pt atom and appears as a protrusion. In Figure 6, the left panels show a series of images revealing H hopping on the p(2 × 2)-N/Pt(111) surface, while the right panels show the corresponding models. In the top image, several H atoms are present on the p(2 × 2)-N layer, where blue and white circles superimposed in the middle of the image indicate the (2 × 2) lattice of N and Pt, respectively. Only the Pt lattice (white circles) is used in Figure 6b−d in order to provide a better view. The tip was placed over the H atom in the middle of the image, shown in Figure 6a, where a pulse (−0.24 V and 1.0 nA for 4 s) was applied. As a result, the H atom hops along the (2 × 2)-Pt and moves to the nearest atop site (shown in Figure 6b). Applying pulses to the same H atom results in a series of hops, and each hop moves the H atom along the (2 × 2)-Pt lattice to the nearest empty atop site. Hops are found to proceed with equal probability in all three directions. However, if the Pt atom is already occupied by a H atom, the target H atom hops to a nearby empty atop site.

Experimental data (blue squares) and the fitted spectrum (blue curve) are shown in Figure 6e for H atom hopping, wherein a threshold is observed at
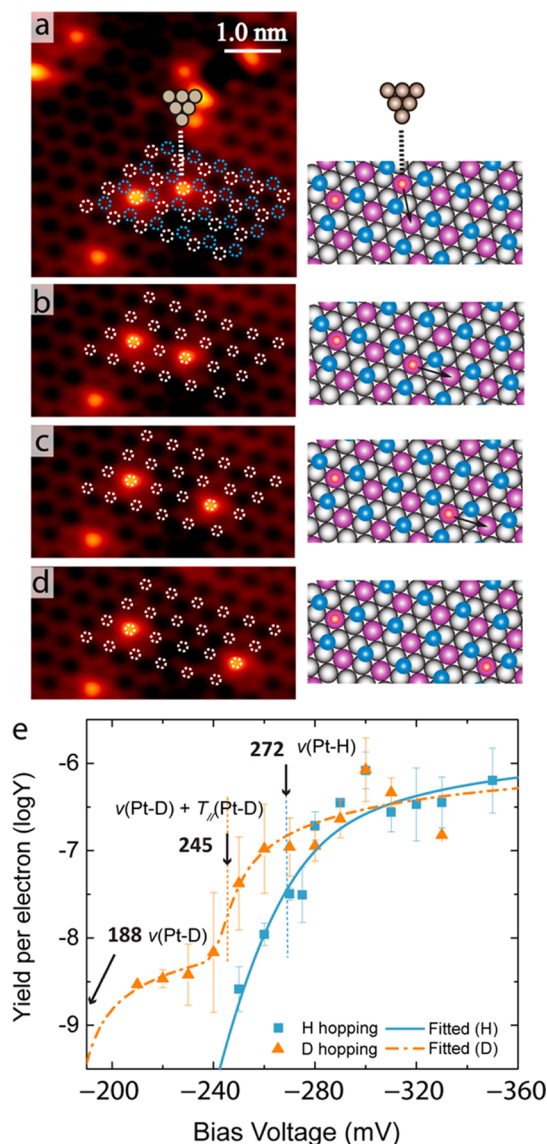

Figure 6. (a−d) Left panel: STM image of H hopping. Blue and white circles indicate the p(2 × 2)-N and Pt(2 × 2) lattices, respectively (5 nm × 5 nm, V_s = 50 mV, I_t = 0.5 nA). Right panel: Models corresponding to each image. (e) Action spectra of H (blue)/D (orange) hopping. Gray, Pt-invisible; purple, Pt-visible; blue, N atom; red, H atom.

272 meV. Compared to the values of the normal modes of H on Pt(111), 276 meV for the Pt−H stretch (v(Pt−H)), and 46 meV for the frustrated translation,[40] the hopping is mediated by v(Pt−H). Substituting H with D, we show the action spectrum for D hopping as the orange triangles and curve in Figure 6e. The fitted curve again has two thresholds, at 188 and 245 meV. The vibrational mode associated with 188 meV is the Pt−D stretch (v(Pt−D)), with an isotopic shift of −84 meV compared to v(Pt−H). The value of 245 meV corresponds to a combination mode of stretch and frustrated translation (v(Pt−D) + $T_∥$(Pt−D)).

Discussion of the Mechanism. In addition to assigning the vibrational modes that are responsible for the motion observed, with the fitted action spectra, we
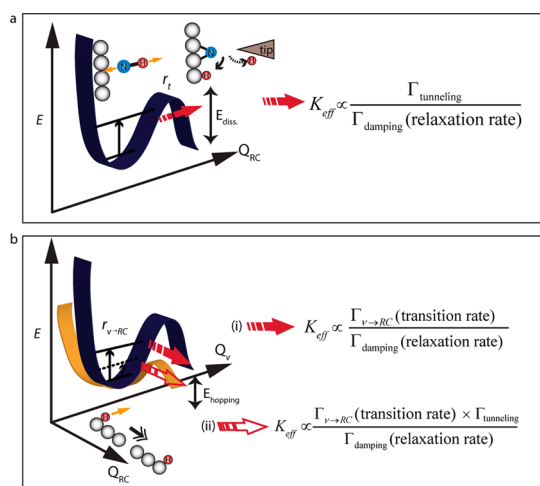
Figure 7. Schematic drawing of the mechanism of (a) NH-(ND) dissociation and (b) H(D) hopping.

can determine the effective prefactor, K_{eff}, which is the branching ratio determined by the rate of the elementary processes involved. Fittings of the action spectra are conducted using the model developed by Motobayashi et al.[15] The relationship between the effective prefactor K_{eff} and the rates of elementary processes has been discussed in detail by Frederiksen and co-authors,[16] and we applied their ideas to our specific cases. Both action spectra were fitted under the scenario of one-electron processes, where the number of electrons involved was determined from the current dependence measurement. As shown in Figure 5g, a clear suppression in the reaction yield is observed for ND dissociation. The K_{eff} determined by the fitted spectra are $10^{-7.23}$ (NH diss.) and $10^{-9.35}$ (ND diss.). Therefore, the calculated value of the kinetic isotope effect (KIE) is, $K_{eff}(NH)/K_{eff}(ND) \approx 10^{-7.23}/10^{-9.35} = 132$. Such a large value indicates that tunneling is involved, which accounts for the suppression of the reaction probability when D is substituted for H. Because the excited NH stretching mode is along the reaction coordinate and the NH dissociation barrier was found to be 1.1 eV,[29] the mechanism involves direct excitation of the NH(ND) stretching mode, followed by tunneling through the barrier, as shown in Figure 7a. In this case, the effective prefactor K_{eff} is proportional to the ratio of the rate of tunneling to the rate of damping.[16] Vibrations at metal surfaces are generally assumed to be damped by electron–hole pair excitation, and early estimates of the damping rates were in the range of 10^{12} to 10^{13} s^{-1}.[41] One experimental way of assessing the damping rates is from vibrational line widths, which place an upper limit on the rate if the line widths are assumed to be dominated by lifetime broadening. The line width of the N–H stretch of NH on Pt(111) depends on coverage but at the highest coverage has an intrinsic full width at half-maximum (fwhm) as narrow as 4 cm^{-1},[28] implying that the

damping rate can be no greater than 8×10^{11} s^{-1}. If we make the reasonable assumption that even at its narrowest measured value, there is still some contribution to the fwhm from inhomogeneous broadening, the contribution to the fwhm from lifetime broadening is likely no greater than about 1 cm^{-1}, which is the width of the narrowest vibrational lines of adsorbates on metal surfaces. Thus, we assume a damping rate $\Gamma_{damping}$ of 10^{11} s^{-1}. Using this value for $\Gamma_{damping}$ and an effective prefactor $K_{eff}(NH)$ for NH dissociation of $10^{-7.23}$ yields an estimated tunneling rate for NH dissociation of $\approx 6 \times 10^3$ s^{-1}, while for ND dissociation, the rate of tunneling is ≈ 45 s^{-1}.

H(D) hopping differs from NH(ND) dissociation as the activated mode is not along the reaction coordinate (parallel to the surface in the case of hopping). Thus, a different mechanism is proposed, as shown in Figure 7b. Two cases are considered. The solid arrow in Figure 7b shows the mechanism when the excitation energy is greater than the hopping barrier, which accounts for H(D) hopping with energy greater than 245 meV. The calculated value of the KIE is given by $K_{eff}(H)/K_{eff}(D) \approx 10^{-5.55}/10^{-5.8} = 1.78$. Comparable rates for H and D hopping indicate that the activation energy is sufficient to overcome the hopping barrier, where the Pt–H(D) stretch is first excited by tunneling electrons and its energy is dissipated to the frustrated translation mode via anharmonic coupling. In such a case, the observed effective prefactor K_{eff} is proportional to the ratio of the rate of intermode transition to the rate of damping (eq (i) in Figure 7b). Similarly, by assuming a damping rate of 10^{11} s^{-1}, the intermode transition rate is estimated to be 3×10^5 and 1.6×10^5 s^{-1} for H and D, respectively. The second case is indicated by the open arrow in Figure 7b, where the excitation energy is lower than the reaction barrier. When reducing the bias voltage to a value lower than 245 mV, the tunneling electrons that cannot excite the ν(Pt–H) mode excite the ν(Pt–D) mode. Coupling of ν(Pt–D) to the frustrated translation mode excites $T_\parallel$(Pt–D) from the vibrational ground state to a higher level but with energy below the hopping barrier, and tunneling is required for the excited D to hop to the next site. The reaction rate thus must include an additional term for tunneling. As shown in Figure 7b, eq (ii), the effective prefactor K_{eff} is proportional to $(\Gamma_{\nu \to RC} \times \Gamma_t)/\Gamma_{damping}$. A numerical value of 0.016 s^{-1} is obtained for Γ_t (the rate of D tunneling through the hopping barrier), by assuming 10^{11} s^{-1} for $\Gamma_{damping}$ (e–h excitation), 1.6×10^5 s^{-1} for $\Gamma_{\nu \to RC}$ (obtained as described earlier), and $10^{-7.6}$ for K_{eff} (determined from the action spectrum fits). With our observation of the hopping of D atoms with energies above and below the barrier, the hopping barrier for D on p(2 × 2)-N/Pt(111) is estimated to be between 188 and 245 meV. Table 1 summarizes the fitted parameters of the action spectra, which include the corresponding vibrational

TABLE 1. Summary of the Fitted Vibrational Energy (Ω), Broadening Factor (γ), Effective Prefactor (K_{eff}), Corresponding Vibrational Modes, and Estimated Rates of the Corresponding Elementary Process

fitted parameter for AS	Ω (meV)	K_{eff}	γ (meV)	corresponding vibrational modes	rate (s^{-1})	(process)
NH dissociation	430	$10^{-7.23}$	15	$\nu_s(N-H)$	6×10^3	($\Gamma_{tunneling}$)
ND dissociation	745 (Ω_2)	$10^{-7.6}$	6	$2\nu_s(N-D) + L(N-D)$	2.5×10^3	($\Gamma_{tunneling}$)
	320 (Ω_1)	$10^{-9.35}$	4	$\nu_s(N-D)$	45	($\Gamma_{tunneling}$)
H hopping	272	$10^{-5.55}$	13	$\nu(Pt-H)$	3×10^5	($\Gamma_{\nu \rightarrow RC}$)
D hopping	245 (Ω_2)	$10^{-5.8}$	4	$\nu(Pt-D) + T_{\parallel}(Pt-D)$	1.6×10^5	($\Gamma_{\nu \rightarrow RC}$)
	188 (Ω_1)	$10^{-7.6}$	4	$\nu(Pt-D)$	0.016	($\Gamma_{tunneling}$)

modes, the elementary processes that account for the motions, and the estimated rates.

CONCLUSION

Atomic-scale details of a simple hydrogenation reaction, N + H → NH, are revealed by LT-STM. By altering the electronic properties of neighboring Pt atoms, once formed, an NH molecule inhibits further hydrogenation of nearby N atoms. A mechanism is proposed to explain the presence of both isolated NH molecules and dense (2 × 2) islands of NH. The surface morphologies of H and NH on N-covered Pt(111) are favorable for atomic-scale manipulation. The well-ordered p(2 × 2)-N layer constrains the occupancy of H atoms to the lattice of Pt atop sites. Action spectra corresponding to dissociation of NH(ND) molecules and hopping of H(D) atoms reveal that both processes are vibrationally mediated. Fitting of the spectra to a theoretical model allows key parameters of the dynamics to be extracted from the data. Comparison of the parameters for NH dissociation with those of ND reveals that tunneling of the H atom through the dissociation barrier plays an important role in NH dissociation.

METHODS

The experiments were carried out in linked ultrahigh vacuum STM and preparation chambers as described in an earlier publication.[42] Base pressures of the STM and preparation chambers were 1×10^{-11} Torr and 1×10^{-9} Torr, respectively. STM images were obtained at 4.7 K with an Omicron low-temperature scanning probe microscope (LT-SPM) system. Omicron SCALA PRO 4.0 software was used for data acquisition. Image processing was carried out with the WSxM program provided by Nanotec.[43] Cleaning of the Pt(111) crystal follows the same procedure described in an earlier publication.[42] Briefly, the sample was cleaned by 5−8 cycles of annealing (held at 1220 K for 10 min by e-beam heating) and sputtering (at 300 K), followed by O_2 exposure (1×10^{-7} Torr) at 750 K for 10 min and flash annealing to 1220 K. Sputtering was performed with an argon pressure of 3×10^{-5} Torr and an Ar$^+$ energy of 1000 eV. Surface cleanness was verified by STM and occasionally by LEED. The nitrogen-covered Pt surface was prepared *via* the oxydehydrogenation of NH_3, which has been described in detail in the experimental section of ref 18. Briefly, the surface was saturated with molecular O_2 and then exposed to NH_3 at 50 K. After that, the NH_3-O_2-covered surface was transferred to a heating stage and heated to the target temperature and held there for 60 s. The annealing temperature was accurately controlled on the heating stage by a thermocouple mounted on the sample. H_2 gas was then admitted to the STM chamber (1.0×10^{-10} Torr for 20 s) with the sample at 50 K before obtaining the images of H adsorption shown in Figure 1. The NH layer at high coverage was formed by exposing the N-covered surface to H_2 gas while the sample was held at 300 K. H_2 gas was introduced *via* a nozzle (5.0×10^{-9} Torr for 120 s, repeated 7 times). Twenty minute intervals between each exposure were used for recovering the background pressure, with a total of 140 min to finish the exposure. All STM images were acquired after the sample was cooled back to 4.7 K.

Conflict of Interest: The authors declare no competing financial interest.

Supporting Information Available: Additional STM images showing NH_3 and NH obtained under different conditions along with additional models of adsorbate structure are provided. The Supporting Information is available free of charge on the ACS Publications website at DOI: 10.1021/acsnano.5b02774.

REFERENCES AND NOTES

1. Binnig, G.; Rohrer, H. Scanning Tunneling Microscopy. *Surf. Sci.* **1983**, *126*, 236–244.
2. Binnig, G.; Rohrer, H.; Gerber, C.; Weibel, E. Tunneling through a Controllable Vacuum Gap. *Appl. Phys. Lett.* **1982**, *40*, 178–180.
3. Tatarkhanov, M.; Rose, F.; Fomin, E.; Ogletree, D. F.; Salmeron, M. Hydrogen Adsorption on Ru(0001) Studied by Scanning Tunneling Microscopy. *Surf. Sci.* **2008**, *602*, 487–492.
4. Mitsui, T.; Rose, M. K.; Fomin, E.; Ogletree, D. F.; Salmeron, M. Hydrogen Adsorption and Diffusion on Pd(111). *Surf. Sci.* **2003**, *540*, 5–11.
5. Lauhon, L. J.; Ho, W. Direct Observation of the Quantum Tunneling of Single Hydrogen Atoms with a Scanning Tunneling Microscope. *Phys. Rev. Lett.* **2000**, *85*, 4566–4569.
6. Fernández-Torres, L. C.; Sykes, E. C. H.; Nanayakkara, S. U.; Weiss, P. S. Dynamics and Spectroscopy of Hydrogen Atoms on Pd(111). *J. Phys. Chem. B* **2006**, *110*, 7380–7384.
7. Mii, T.; Tikhodeev, S. G.; Ueba, H. Spectral Features of Inelastic Electron Transport *Via* a Localized State. *Phys. Rev. B: Condens. Matter Mater. Phys.* **2003**, *68*, 205406.
8. Ueba, H.; Mii, T.; Tikhodeev, S. G. Theory of Inelastic Tunneling Spectroscopy of a Single Molecule − Competition between Elastic and Inelastic Current. *Surf. Sci.* **2007**, *601*, 5220–5225.
9. Mii, T.; Tikhodeev, S.; Ueba, H. Theory of Vibrational Tunneling Spectroscopy of Adsorbates on Metal Surfaces. *Surf. Sci.* **2002**, *502−503*, 26–33.
10. Jewell, A. D.; Peng, G.; Mattera, M. F. G.; Lewis, E. A.; Murphy, C. J.; Kyriakou, G.; Mavrikakis, M.; Sykes, E. C. H. Quantum Tunneling Enabled Self-Assembly of Hydrogen Atoms on Cu(111). *ACS Nano* **2012**, *6*, 10115–10121.

11. Hla, S.-W. Scanning Tunneling Microscopy Single Atom/ Molecule Manipulation and Its Application to Nanoscience and Technology. *J. Vac. Sci. Technol., B: Microelectron. Process. Phenom.* **2005**, *23*, 1351–1360.

12. Sainoo, Y.; Kim, Y.; Okawa, T.; Komeda, T.; Shigekawa, H.; Kawai, M. Excitation of Molecular Vibrational Modes with Inelastic Scanning Tunneling Microscopy Processes: Examination through Action Spectra of *cis*-2-Butene on Pd(110). *Phys. Rev. Lett.* **2005**, *95*, 246102.

13. Kim, Y.; Motobayashi, K.; Frederiksen, T.; Ueba, H.; Kawai, M. Action Spectroscopy for Single-Molecule Reactions — Experiments and Theory. *Prog. Surf. Sci.* **2015**, *90*, 85–143.

14. Ueba, H.; Persson, B. N. J. Action Spectroscopy for Single-Molecule Motion Induced by Vibrational Excitation with a Scanning Tunneling Microscope. *Phys. Rev. B: Condens. Matter Mater. Phys.* **2007**, *75*, 041403.

15. Motobayashi, K.; Kim, Y.; Ueba, H.; Kawai, M. Insight into Action Spectroscopy for Single Molecule Motion and Reactions through Inelastic Electron Tunneling. *Phys. Rev. Lett.* **2010**, *105*, 076101.

16. Frederiksen, T.; Paulsson, M.; Ueba, H. Theory of Action Spectroscopy for Single-Molecule Reactions Induced by Vibrational Excitations with STM. *Phys. Rev. B: Condens. Matter Mater. Phys.* **2014**, *89*, 035427.

17. Stipe, B. C.; Rezaei, M. A.; Ho, W. Atomistic Studies of O_2 Dissociation on Pt(111) Induced by Photons, Electrons, and by Heating. *J. Chem. Phys.* **1997**, *107*, 6443–6447.

18. Liang, Z.; Jin Yang, H.; Kim, Y.; Trenary, M. Surface Morphology of Atomic Nitrogen on Pt(111). *J. Chem. Phys.* **2014**, *140*, 114707.

19. Ludwig, J.; Vlachos, D. G. Molecular Dynamics of Hydrogen Dissociation on an Oxygen Covered Pt(111) Surface. *J. Chem. Phys.* **2008**, *128*, 154708.

20. Michaelides, A.; Hu, P. Catalytic Water Formation on Platinum: A First-Principles Study. *J. Am. Chem. Soc.* **2001**, *123*, 4235–4242.

21. Kresse, G.; Furthmüller, J. Efficient Iterative Schemes for *Ab Initio* Total-Energy Calculations Using a Plane-Wave Basis Set. *Phys. Rev. B: Condens. Matter Mater. Phys.* **1996**, *54*, 11169–11186.

22. Kresse, G.; Hafner, J. Ab Initio Molecular Dynamics for Liquid Metals. *Phys. Rev. B: Condens. Matter Mater. Phys.* **1993**, *47*, 558–561.

23. Blöchl, P. E. Projector Augmented-Wave Method. *Phys. Rev. B: Condens. Matter Mater. Phys.* **1994**, *50*, 17953–17979.

24. Kresse, G.; Joubert, D. From Ultrasoft Pseudopotentials to the Projector Augmented-Wave Method. *Phys. Rev. B: Condens. Matter Mater. Phys.* **1999**, *59*, 1758–1775.

25. Perdew, J. P.; Burke, K.; Ernzerhof, M. Generalized Gradient Approximation Made Simple. *Phys. Rev. Lett.* **1996**, *77*, 3865–3868.

26. Tersoff, J.; Hamann, D. R. Theory and Application for the Scanning Tunneling Microscope. *Phys. Rev. Lett.* **1983**, *50*, 1998–2001.

27. Tersoff, J.; Hamann, D. R. Theory of the Scanning Tunneling Microscope. *Phys. Rev. B: Condens. Matter Mater. Phys.* **1985**, *31*, 805–813.

28. Herceg, E.; Jones, J.; Mudiyanselage, K.; Trenary, M. Formation and Hydrogenation of p(2 × 2)-N on Pt(111). *Surf. Sci.* **2006**, *600*, 4563–4571.

29. Mudiyanselage, K.; Trenary, M.; Meyer, R. J. Kinetics of NH Formation and Dissociation on Pt(111). *J. Phys. Chem. C* **2007**, *111*, 7127–7136.

30. Christmann, K.; Ertl, G.; Pignet, T. Adsorption of Hydrogen on a Pt(111) Surface. *Surf. Sci.* **1976**, *54*, 365–392.

31. Herceg, E.; Mudiyanselage, K.; Trenary, M. Reversible Hydrogenation of Surface N Atoms to Form NH on Pt(111). *J. Phys. Chem. B* **2005**, *109*, 2828–2835.

32. Shi, H.; Jacobi, K.; Ertl, G. Interaction of Hydrogen with Nitrogen Atoms Chemisorbed on a Ru(0001) Surface. *J. Chem. Phys.* **1995**, *102*, 1432–1439.

33. Kiskinova, M.; Goodman, D. W. Interaction of H_2 and CO with Carbided and Nitrided Ni(100). *Surf. Sci.* **1981**, *109*, L555–L559.

34. Tsai, W.; Vajo, J. J.; Weinberg, W. H. Perturbations in the Surface Chemistry of Hydrogen by Nitrogen Adatoms on Platinum(110)-(1 × 2). *J. Phys. Chem.* **1988**, *92*, 1245–1251.

35. Verheij, L. K.; Hugenschmidt, M. B. Hydrogen Adsorption on Oxygen Covered Pt(111). *Surf. Sci.* **1995**, *324*, 185–201.

36. McCormack, D. A.; Olsen, R. A.; Baerends, E. J. Mechanisms of H_2 Dissociative Adsorption on the Pt(211) Stepped Surface. *J. Chem. Phys.* **2005**, *122*, 194708.

37. Salanov, A. N.; Bibin, V. N.; Rudina, N. A. Island Formation in Chemisorption 1. Chemisorption Model. *React. Kinet. Catal. Lett.* **1998**, *64*, 261–268.

38. Salanov, A. N.; Bibin, V. N.; Rudina, N. A. Island Formation in Chemisorption 2. Chemisorption Kinetics. *React. Kinet. Catal. Lett.* **1998**, *64*, 269–274.

39. Michaelides, A.; Hu, P. Insight into Microscopic Reaction Pathways in Heterogeneous Catalysis. *J. Am. Chem. Soc.* **2000**, *122*, 9866–9867.

40. Offermans, W. K.; Jansen, A. P. J.; van Santen, R. A. Ammonia Activation on Platinum (111): A Density Functional Theory Study. *Surf. Sci.* **2006**, *600*, 1714–1734.

41. Persson, M.; Hellsing, B. Electronic Damping of Adsorbate Vibrations on Metal Surfaces. *Phys. Rev. Lett.* **1982**, *49*, 662–665.

42. Liang, Z.; Kim, H.; Kim, Y.; Trenary, M. Molecular Oxygen Network as a Template for Adsorption of Ammonia on Pt(111). *J. Phys. Chem. Lett.* **2013**, *4*, 2900–2905.

43. Horcas, I.; Fernandez, R.; Gomez-Rodriguez, J. M.; Colchero, J.; Gomez-Herrero, J.; Baro, A. M. Wsxm: A Software for Scanning Probe Microscopy and a Tool for Nanotechnology. *Rev. Sci. Instrum.* **2007**, *78*, 013705.